International Journal of Analysis and Applications

Numerical Simulation of Phycoremediation for Nutrient Removal Using the Extended Monod Model with Saulyev Technique

Areerat Vongkok[1], Anantanit Chumsri[1,*], Nopparat Pochai[2,3]

[1]*Faculty of Science and Fisheries Technology, Rajamangala University of Technology Srivijaya, Trang Campus, Trang 92150, Thailand*

[2]*Faculty of Science, King Mongkut's Institute of Technology Ladkrabang, Bangkok 10520, Thailand*

[3]*Centre of Excellence in Mathematics, CHE, Si Ayutthaya Road, Bangkok 10400, Thailand*

**Corresponding author:* anantanit.p@rmutsv.ac.th

ABSTRACT. Nowadays, as water pollution is increasing from agricultural sectors due to nitrogen and phosphorus, phycoremediation is used to remove nutrients with microalgae. In this paper, a mathematical model is developed to use the extended Monod model to analyze the growth of microalgae that have adsorbed nutrients by considering various flow velocities and levels of nitrogen as effects of biomass concentration. This model has been calculated with the numerical finite difference method using the Saulyev technique. Numerical simulations show results for various scenarios with flow velocities and levels of nitrogen that affect the growth of microalgae.

1. Introduction

These days, one of the most significant environmental problems facing the government and scientists is water contamination. As more organic and inorganic compounds are released into the environment, especially surface water sources such as lakes, ponds, rivers, and oceans, which is home to various plant and animal species that rely on both the amount and quality of the water to exist, is affected [1,2]. Since diffuse sources, primarily agriculture, account for three-quarters of global nitrogen (N) water pollution, agriculture continues to be one of the major contributors to water pollution with fertilizers and pesticides [1]. In Organization for Economic

Received Sep. 28, 2025

2020 Mathematics Subject Classification. 92D25.

Key words and phrases. extended Monod model; Saulyev technique; nutrient.

https://doi.org/10.28924/2291-8639-24-2026-39

ISSN: 2291-8639

Co-operation and Development (OECD) countries, it was found that between 20 and 80 percent of nitrogen (N) and phosphorus (P), which contaminated surface water sources, are derived from agricultural sections [3] such as fertilizers, which were the first source of contaminants [4]. According to evidence from Statista, the global consumption of agricultural fertilizers containing nitrogen and phosphorus has steadily risen from 1965 to 2022. Nitrogen fertilizer demand has increased dramatically on a global scale. It was noted that usage of phosphorus fertilizers was also on the rise, albeit at a slower rate than that of nitrogen, as shown in Figure 1 [5,6]. In addition, runoff from agriculture comprises excess water from rainfall and irrigation [3]. This runoff frequently contains a variety of pollutants that contribute to agricultural water pollution, including pesticide leaching, nutrient runoff, and poor livestock waste management. These pollutants lead to high levels of phosphorus and nitrogen, which can cause eutrophication and the development of toxic algal blooms that deplete oxygen and kill fish. Additionally, it may contaminate drinking water, harm aquatic life [7], and cause adverse health effects like cancer, thyroid and neural tube abnormalities, diabetes, and blue baby syndrome (methemoglobinemia) [8].

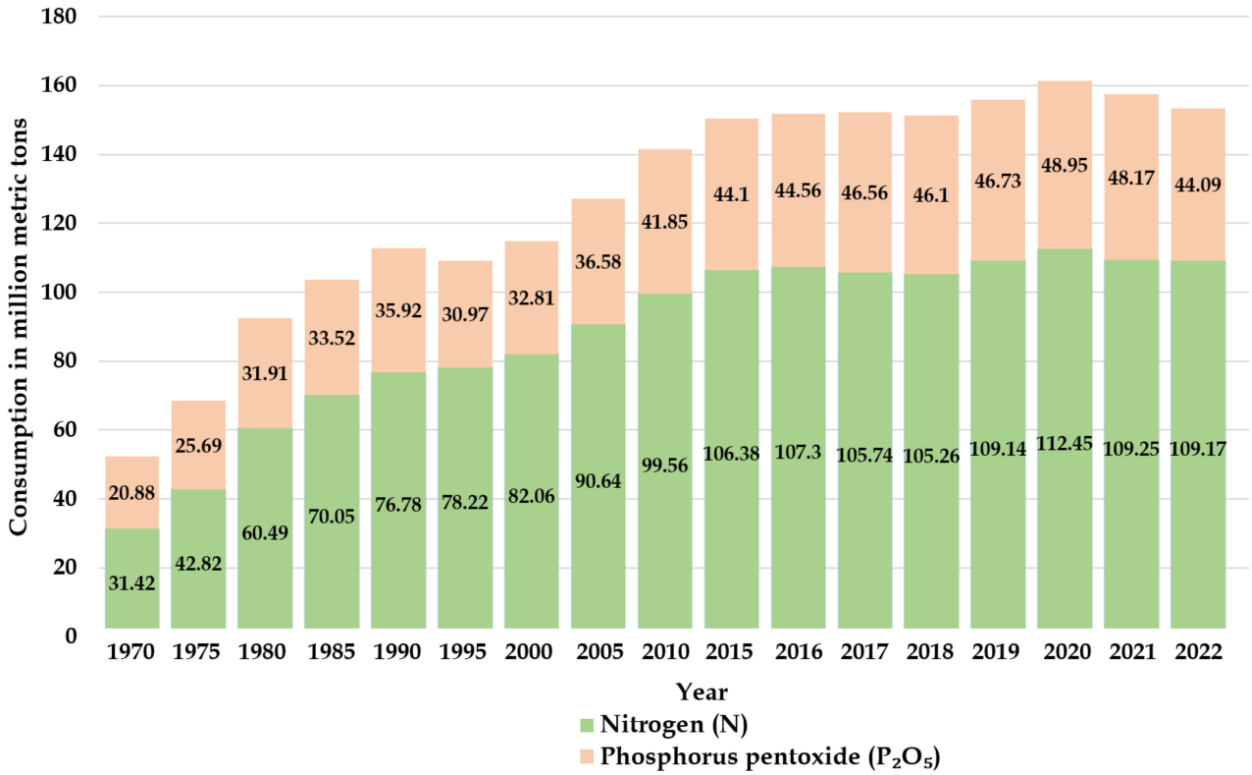

Figure 1. Global consumption of agricultural fertilizers from 1965 to 2022, by nutrient (N and P_2O_5), in million metric tons.

Protection of water sources and quality is imperative due to severe water pollution and the worldwide shortage of water resources. People must be educated about the environment and the harmful impacts of water pollution to stop these negative effects [2]. One appropriate and long- term strategy for addressing environmental problems associated with diffuse water pollution from agriculture is the application of nature-based solutions (NBSs). Utilizing natural mitigating processes, NBSs can facilitate the recovery of otherwise lost resources (such as nutrients) and aid in the removal of various toxins from agricultural wastewater such as nitrogen affects various habitats among these. However, a variety of decontamination processes exist, such as plant uptake, microbial degradation, substrate adsorption and filtration, precipitation, sedimentation, and volatilization [9]. The bioremediation method is one of the NbS that has the potential for treating wastewater that uses microorganisms like microalgae; it is called phycoremediation [10]. Microalgae are known to be pollution scavengers for various substances and have demonstrated significant promise in eliminating pollutants from wastewater. According to the experimental investigation, *Botryococcus* sp. demonstrated a favorable outcome in the phycoremediation treatment of wastewater by slowing down the rate of nutrient infiltration and enabling efficient growth. Because microalgae can collect and transform wastewater nutrients into biomass, biomass was produced during phycoremediation [1].

Mathematical modeling is an important tool for understanding the dynamics of behavior, involving physical, chemical, biological, and other processes, which can be made possible, which can also be used to simulate the effects of various scenarios under various environmental conditions and to examine the way environmental problem-solving works. Partial differential equations are one of the most practical methods for numerically simulating system dynamics, and one example is the advection-diffusion equation, which models diffusion and transport issues [11] as in [12]-[17]. To solve the equations for numerical approximation and guarantee correctness, the finite difference method uses numerical techniques. This scheme of the Saulyev technique is its explicitness and unconditional stability [18] that is the best option for real-world applications of models with somewhat large time steps since numerical solutions are consistent, monotonic, robust, and efficient [19] in accurately approximating solutions across the provided interval. There are research studies that have conducted mathematical modeling that are solving partial differential equations using the Saulyev technique, such as In [20], FTCS and the Saulyev technique are used in this one-dimensional mathematical model of river salinity assessment that takes into account the impacts when fresh water comes from the barrage dam. The Saulyev

technique yields precise approximations and ensures a stable solution across any grid spacing. In [21], using the Saulyev technique, a straightforward numerical simulation of advection-dispersion-reaction processes is shown. By taking into account the maximum concentration level, it is impacted by increasing the mass decaying rate, which is a good approximation. In [22], conducting the approximate conceptual design of the shoreline evolution in each year and over an extended period of time, they use the FTCS and Saulyev techniques to perform a non-dimensional shoreline evolution model with a groin structure model that takes groin structural impacts into account. In situations where the number of grids has increased, the Saulyev technique can be quite beneficial.

The majority of microalgae growth models rely on modified Monod kinetics, which frequently require the identification of several parameters. Temperature, water pH, light intensity, and nutrition availability all have an impact on microalgae growth. One of the most effective models for describing the direct correlation between a certain growth rate and the concentration of a critical substrate is the Monod equation. All of these variables that affect microalgae development are taken into account by the Monod model, which is used to calculate microalgae growth [23].

The main aim of this paper is to establish a mathematical model to explain the development of microalgae in the stream. We provide a one-dimensional advection-dispersion-reaction equation, a dynamic behavior model of microalgae development that uses the Saulyev technique-based finite difference method to account for scenarios of biomass concentrations of *Botryococcus* sp., which consider nitrogen levels in agricultural wastewater areas that affect microalgae growth. For this model, we run five simulations that examine its dependence on various nitrogen levels and flow velocities using parameters from laboratory experiments and the findings of a numerical analysis. We conduct a comparison and discussion of the breakthrough concentration curves acquired for the various circumstances.

2. Dispersion model

Here we propose a simple one-dimensional spatial-temporal model that shows biomass concentrations in a stream. We focus on the growth of microalgae for agricultural wastewater.

This process can be explained using an advection-diffusion-reaction equation and the specific growth rate, which extends the Monod model that relates nitrogen, phosphorus, and light intensity [23] as follows:

$$\frac{\partial C_m(x,t)}{\partial t} = -u\frac{\partial C_m(x,t)}{\partial x} + D\frac{\partial^2 C_m(x,t)}{\partial x^2} + MC_m(x,t)e^{\mu t} - mC_m(x,t), \quad 0 \le x \le L, 0 < t \le T, \tag{2.1}$$

where $\mu(x,t) = \mu_{\max}\left[\frac{C_n}{K_n + C_n}\right]\left[\frac{C_p}{K_p + C_p}\right]\left[\frac{I}{K_I + I}\right]$

the initial condition

$$C_m(x,0) = f(x), \quad 0 \le x \le L, \tag{2.2}$$

and the boundary condition

$$\begin{aligned} C_m(0,t) &= g(t), \quad 0 \le t \le T, \\ \frac{\partial C_m(L,t)}{\partial x} &= h(t), \quad 0 \le t \le T, \end{aligned} \tag{2.3}$$

where parameters of this model describe meanings, as

x	space (m)
t	time (d)
$\mu_{\max}$	the maximum specific growth rate of microalgae (d^{-1})
μ	the specific growth rate of microalgae (d^{-1})
K_n	the half saturation constants for nitrogen (mg/L)
K_p	the half saturation constants for phosphorus (mg/L)
K_I	the half saturation constants for light intensity (μ**mol/m^2 s^1**)
C_n	the nitrogen concentration (mg/L)
C_m	the biomass concentration (mg/L)
C_p	the phosphorus concentration (mg/L)
I	the light intensity (μ**mol/m^2 s^1**)
M	the maximal microalgae-specific production rate (d^{-1})
m	the loss rate of microalgae (d^{-1})
u	the water flow velocity of stream (m/s)
D	the microalgae diffusion coefficient (m^2/s)

3. Numerical Techniques

In this section, we examine the numerical scheme of the finite difference method, a popular numerical technique for determining the approximate solutions of an initial and boundary conditions value problem. For the one- dimensional advection- diffusion- reaction equation, we employ Saulyev finite difference techniques.

3.1 Saulyev technique

Asymmetric approximations for parabolic equations, such as advection diffusion equations, which are frequently employed to address environmental challenges, were introduced by Saulyev (1964). The answer is provided as an explicit approximation with unconditional stability [17].

These expressions are Saulyev scheme expansions, which can be written as the discretization derivative terms for time and space, respectively.

Let $C(x,t)$ denote C_i^n then

$$\frac{\partial C}{\partial t} = \frac{C_i^{n+1} - C_i^n}{\Delta t}, \qquad \frac{\partial C}{\partial x} = \frac{C_{i+1}^n - C_{i-1}^{n+1}}{2\Delta x}, \tag{3.1}$$

and $$\frac{\partial^2 C}{\partial x^2} = \frac{C_{i+1}^n - C_i^n - C_i^{n+1} + C_{i-1}^{n+1}}{(\Delta x)^2}.$$

3.2 Applied model with Saulyev technique

The biomass concentrations are approximated by using Saulyev scheme. We can solve C_i^n or $C(x_i,t_n)$ at point (x_i,t_n) where the domain $x \in [0,L]$ and $t \in [0,T]$ are divided into $x_i = i\Delta x$ for all $i = 0,1,2,...,M$ and $t_n = n\Delta t$ for all $n = 0,1,2,...,N$ such that $M, N \in \mathbb{N}$ subintervals with equal length $\Delta x = \frac{L}{M}$ and $\Delta t = \frac{T}{N}$.

$$\frac{(C_m)_i^{n+1} - (C_m)_i^n}{\Delta t} = -u\left(\frac{(C_m)_{i+1}^n - (C_m)_{i-1}^{n+1}}{2\Delta x}\right) + D\left(\frac{(C_m)_{i+1}^n - (C_m)_i^n - (C_m)_i^{n+1} + (C_m)_{i-1}^{n+1}}{(\Delta x)^2}\right) \tag{3.2}$$
$$+M(C_m)_i^n e^{\mu t} - m(C_m)_i^n, \qquad 0 \le x \le L, 0 < t \le T,$$

where $\mu = \mu_{\max}\left[\frac{C_n}{K_n + C_n}\right]\left[\frac{C_p}{K_p + C_p}\right]\left[\frac{I}{K_I + I}\right]$

(3.3) is the result of rearranging (3.2), which is represented as

$$(C_m)_i^{n+1} = \frac{1}{(1+\lambda)}\left(\left(\frac{1}{2}\gamma+\lambda\right)(C_m)_{i-1}^{n+1} + \left(1-\lambda+Me^{\mu t}\Delta t - m\Delta t\right)(C_m)_i^n + \left(\lambda-\frac{1}{2}\gamma\right)(C_m)_{i+1}^n\right) \tag{3.3}$$

where $\mu = \mu_{\max}\left[\frac{C_n}{K_n+C_n}\right]\left[\frac{C_p}{K_p+C_p}\right]\left[\frac{I}{K_I+I}\right]$, $\lambda = \frac{D\Delta t}{(\Delta x)^2}$, and $\gamma = \frac{u\Delta t}{\Delta x}$.

The left boundary condition; $i = 0$,

$$C_m(0,t) = h(t) \tag{3.4}$$

and the right boundary condition; $i = M$,

$$\frac{\partial C_m(L,t)}{\partial x} = \frac{(C_m)_{M+1}^n - (C_m)_{M-1}^{n+1}}{2\Delta x} = k(t). \tag{3.5}$$

Substituting (3.5) into (3.3), the right-side equation gives the following expression for solution:

$$(C_m)_M^{n+1} = \frac{1}{(1+\lambda)}\left(2\lambda(C_m)_{M-1}^{n+1} + \left(1-\lambda+Me^{\mu t}\Delta t - m\Delta t\right)(C_m)_L^n + 2k(t)\Delta x\left(\lambda-\frac{1}{2}\gamma\right)\right) \tag{3.6}$$

where $\mu = \mu_{\max}\left[\frac{C_n}{K_n+C_n}\right]\left[\frac{C_p}{K_p+C_p}\right]\left[\frac{I}{K_I+I}\right]$, $\lambda = \frac{D\Delta t}{(\Delta x)^2}$, and $\gamma = \frac{u\Delta t}{\Delta x}$.

4. Simulation Results

In this section, we simulate numerical computation results that illustrate the growth of microalgae in the stream's aquatic ecosystem by showing biomass concentrations. We determine the various velocities of stream flow and nitrogen levels, which consider how they affect the biomass concentrations. We conducted five simulations using equation (3.6) for our calculations.

Here we assume that the length of the stream and the time are $L = 2$ (200 m) and $T = 1$ (20 d) such that $\Delta x = 0.01$ and $\Delta t = 0.01$. We determine the initial and boundary conditions for the microalgae, and we provide the set of parameter values that follow.

The initial

$$C_m(x,0) = 25, \qquad 0 \le x \le 2 \tag{4.1}$$

and boundary conditions

$$\begin{aligned} &C_m(0,t) = 25 + \exp(t), \qquad 0 < t \le 1, \\ &\frac{\partial C_m(1,t)}{\partial x} = 0\ , \qquad 0 < t \le 1. \end{aligned} \tag{4.2}$$

The values of all biologically reasonable parameters are listed in Table 1.

Table 1. Numerical values of the model's parameters, along with references and estimates.

Symbol	Values	Source	Symbol	Values	Source
$\mu_{\max}$	4.588	[23]	I	300.000	[23]
K_n	328.200	[23]	M	0.990	estimated
K_p	2.413	[23]	m	0.400	estimated
K_I	120.000	[23]	D	0.09	estimated
C_p	267.000	[23]			

4.1 Simulation I

We determine that this stream has the water flow velocity that is possible to follow values of 0.05 m/s, we explore the effect of the nitrogen concentration levels are 20, 300, 600, and 1200 mg/L that append with growth of microalgae.

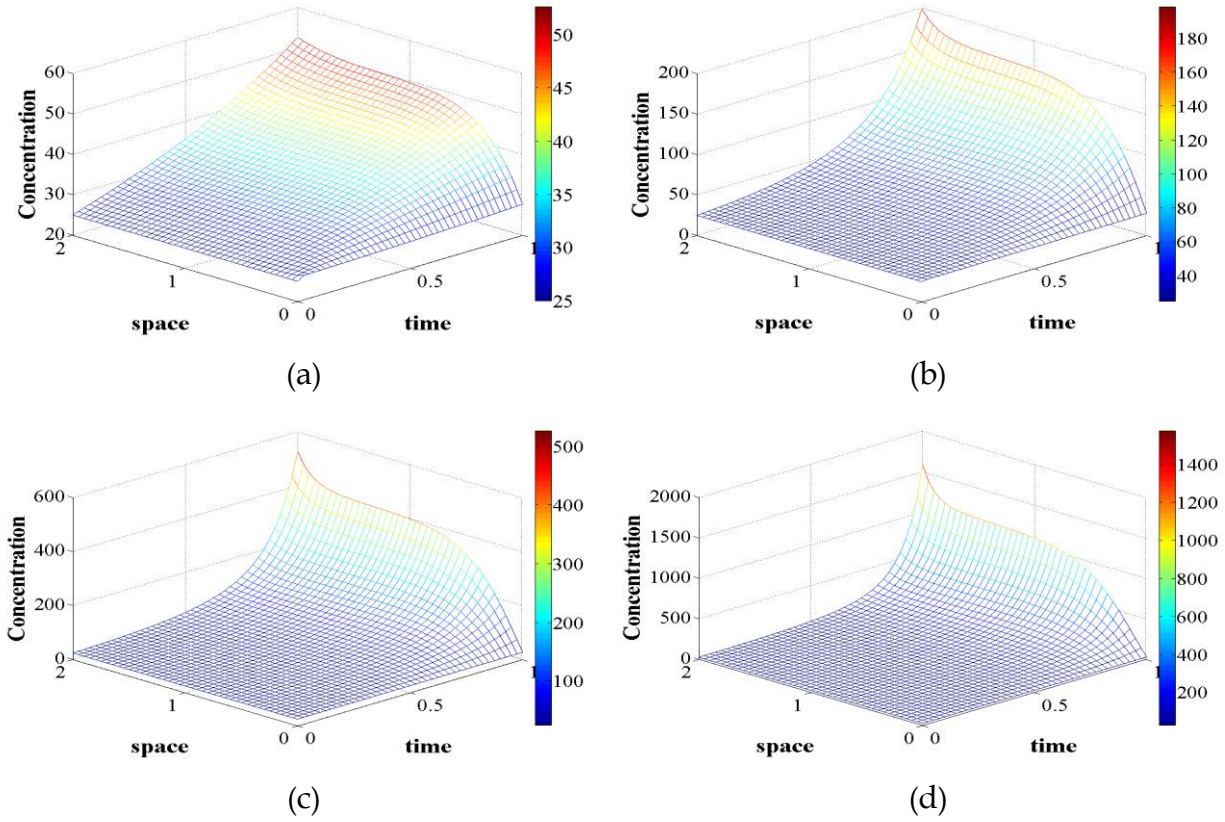

Figure 2. The simulated solution of biomass concentrations (mg/L) at a steam velocity of 0.05 m/s for different nitrogen levels: (a) C_n = 20 mg/L, (b) C_n = 300 mg/L, (c) C_n = 600 mg/L, and (d) C_n = 1200 mg/L.

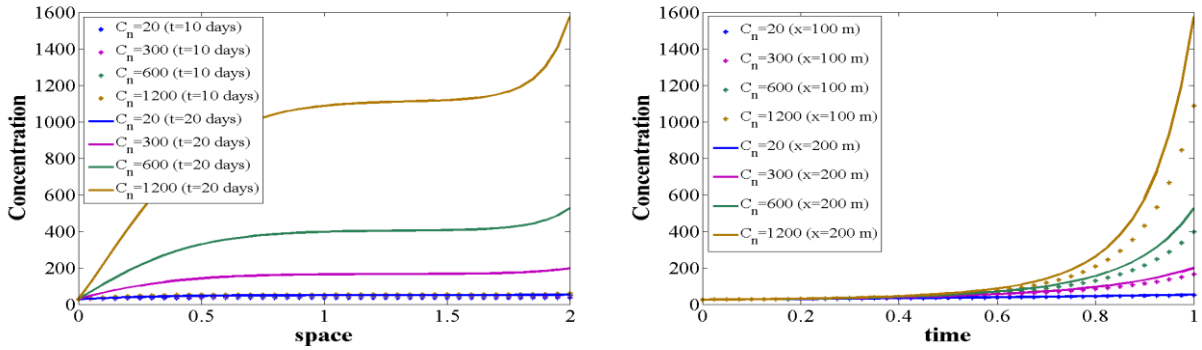

(a) (b)

Figure 3. Comparison of the simulated solutions of biomass concentrations (mg/L) at a steam velocity of 0.05 m/s for different nitrogen levels of 20, 300, 600, and 1200 mg/L through (a) spatial measurements at 10 and 20 d and (b) temporal measurements at 100 and 200 m.

Table 2. The biomass concentrations (mg/L) at a steam velocity of 0.05 m/s for different nitrogen levels of 20 and 300 mg/L.

C_n	**20 mg/L**					**300 mg/L**				
x (m)/ t (d)	**0**	**50**	**100**	**150**	**200**	**0**	**50**	**100**	**150**	**200**
0	25.000	25.000	25.000	25.000	25.000	25.000	25.000	25.000	25.000	25.000
5	26.284	29.119	29.148	29.148	29.872	26.284	30.399	30.443	30.443	31.488
10	26.649	33.964	34.387	34.415	35.655	26.649	41.748	42.558	42.600	45.566
15	27.117	39.598	41.025	41.192	43.021	27.117	68.002	72.522	72.949	81.603
20	27.718	46.279	49.471	49.978	52.562	27.718	142.105	163.823	166.780	198.166

Table 3. The biomass concentrations (mg/L) at a steam velocity of 0.05 m/s for different nitrogen levels of 600 and 1200 mg/L.

C_n	**600 mg/L**					**1200 mg/L**				
x (m)/ t (d)	**0**	**50**	**100**	**150**	**200**	**0**	**50**	**100**	**150**	**2000**
0	25.000	25.000	25.000	25.000	25.000	25.000	25.000	25.000	25.000	25.000
5	26.284	31.015	31.067	31.067	32.273	26.284	31.573	31.632	31.632	32.988
10	26.649	46.737	47.808	47.860	52.103	26.649	52.146	53.515	53.576	59.330
15	27.117	96.159	104.261	104.972	122.634	27.117	138.641	152.863	154.045	188.087
20	27.718	328.148	397.106	406.202	525.278	27.718	851.538	1087.042	1118.158	1575.154

4.2 Simulation II

We determine that this stream has the water flow velocity that is possible to follow values of 0.35 m/s, we explore the effect of the nitrogen concentration levels are 20, 300, 600, and 1200 mg/L that append with growth of microalgae.

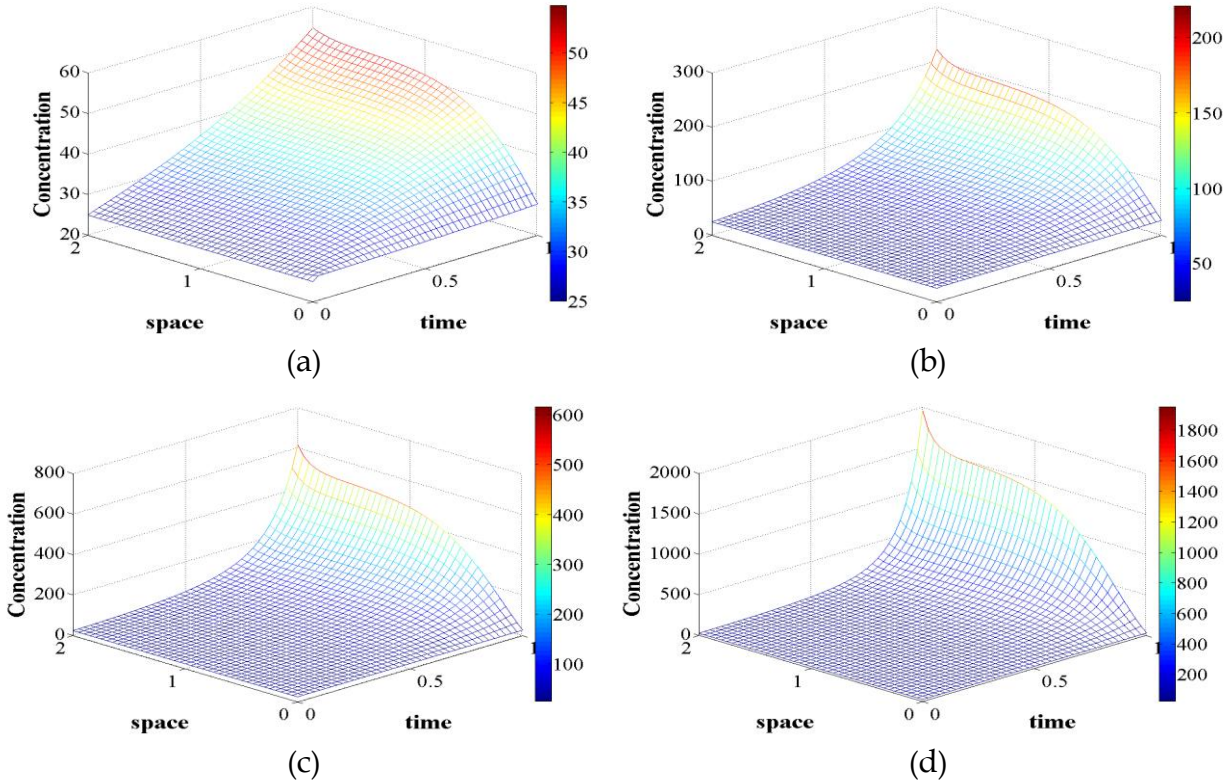

Figure 4. The simulated solution of biomass concentrations (mg/L) at a steam velocity of 0.35 m/s for different nitrogen levels: (a) C_n = 20 mg/L, (b) C_n = 300 mg/L, (c) C_n = 600 mg/L, and (d) C_n = 1200 mg/L.

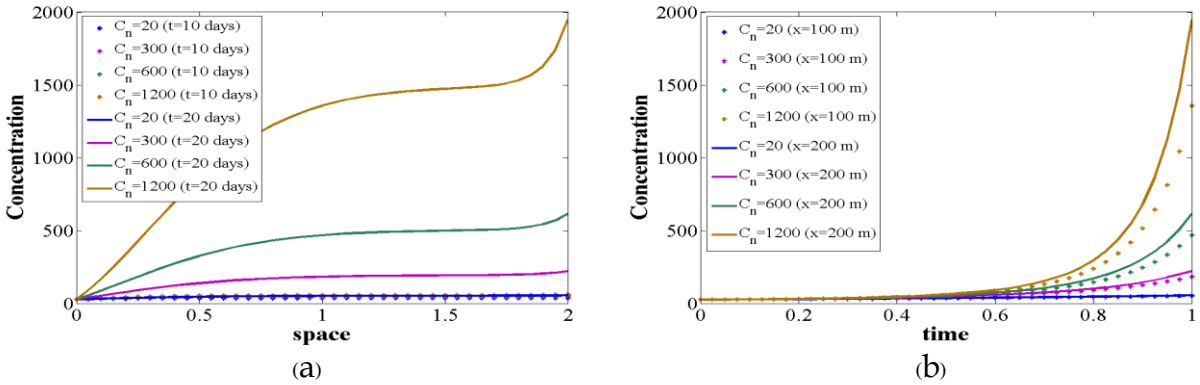

Figure 5. Comparison of the simulated solutions of biomass concentrations (mg/L) at a steam velocity of 0.35 m/s for different nitrogen levels of 20, 300, 600, and 1200 mg/L through (a) spatial measurements at 10 and 20 d and (b) temporal measurements at 100 and 200 m.

Table 4. The biomass concentrations (mg/L) at a steam velocity of 0.35 m/s for different nitrogen levels of 20 and 300 mg/L.

C_n	**20 mg/L**					**300 mg/L**				
x (m)/ t (d)	**0**	**50**	**100**	**150**	**200**	**0**	**50**	**100**	**150**	**200**
0	25.000	25.000	25.000	25.000	25.000	25.000	25.000	25.000	25.000	25.000
5	26.284	29.434	29.515	29.515	30.143	26.284	30.816	30.934	30.935	31.858
10	26.649	34.278	35.252	35.308	36.313	26.649	42.505	44.355	44.457	46.989
15	27.117	39.384	42.421	42.808	44.264	27.117	68.395	78.103	79.280	86.764
20	27.718	44.914	51.248	52.555	54.672	27.718	138.718	183.025	192.108	220.787

Table 5 The biomass concentrations (mg/L) at a steam velocity of 0.35 m/s for different nitrogen levels of 600 and 1200 mg/L.

C_n	**600 mg/L**					**1200 mg/L**				
x (m)/ t (d)	**0**	**50**	**100**	**150**	**200**	**0**	**50**	**100**	**150**	**200**
0	25.000	25.000	25.000	25.000	25.000	25.000	25.000	25.000	25.000	25.000
5	26.284	31.483	31.619	31.620	32.693	26.284	32.089	32.241	32.242	33.454
10	26.649	47.827	50.273	50.406	54.094	26.649	53.633	56.758	56.926	62.001
15	27.117	97.661	115.168	117.301	133.110	27.117	142.391	173.312	177.146	208.582
20	27.718	325.347	468.078	499.124	615.063	27.718	862.200	1356.812	1473.451	1948.896

4.3 Simulation III

We determine that this stream has the water flow velocity that is possible to follow values of 0.65 m/s, we explore the effect of the nitrogen concentration levels are 20, 300, 600, and 1200 mg/L that append with growth of microalgae.

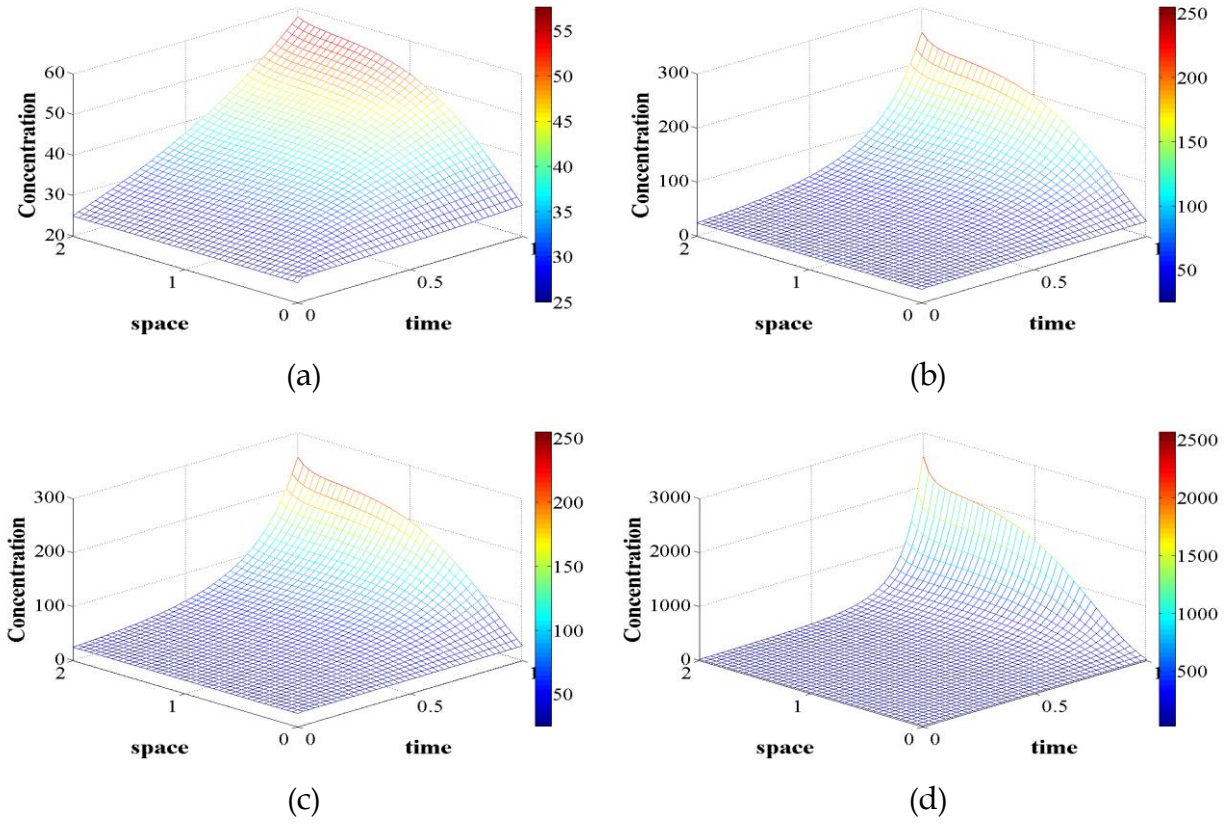

Figure 6. The simulated solution of biomass concentrations (mg/L) at a steam velocity of 0.65 m/s for different nitrogen levels: (a) C_n = 20 mg/L, (b) C_n = 300 mg/L, (c) C_n = 600 mg/L, and (d) C_n = 1200 mg/L.

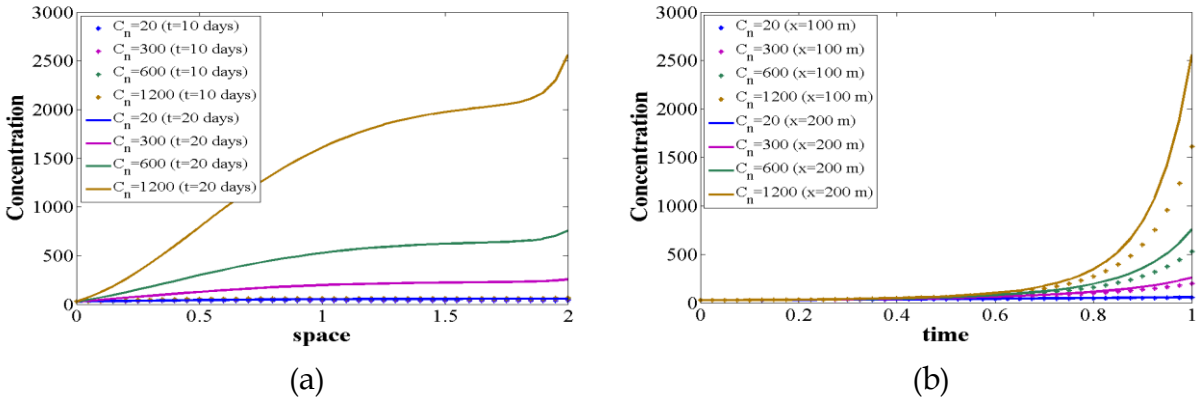

Figure 7. Comparison of the simulated solutions of biomass concentrations (mg/L) at a steam velocity of 0.65 m/s for different nitrogen levels of 20, 300, 600, and 1200 mg/L through (a) spatial measurements at 10 and 20 d and (b) temporal measurements at 100 and 200 m.

Table 6. The biomass concentrations (mg/L) at a steam velocity of 0.65 m/s for different nitrogen levels of 20 and 300 mg/L.

C_n	**20 mg/L**					**300 mg/L**				
x (m)/ t (d)	**0**	**50**	**100**	**150**	**200**	**0**	**50**	**100**	**150**	**200**
0	25.000	25.000	25.000	25.000	25.000	25.000	25.000	25.000	25.000	25.000
5	26.284	29.750	29.951	29.954	30.497	26.284	31.238	31.519	31.524	32.340
10	26.649	34.290	36.186	36.390	37.219	26.649	42.756	46.366	46.742	48.945
15	27.117	38.371	43.511	44.726	46.015	27.117	66.456	83.350	87.176	94.174
20	27.718	42.256	51.703	55.287	57.605	27.718	126.694	196.580	223.102	254.417

Table 7. The biomass concentrations (mg/L) at a steam velocity of 0.65 m/s for different nitrogen levels of 600 and 1200 mg/L.

C_n	**600 mg/L**					**1200 mg/L**				
x (m)/ t (d)	**0**	**50**	**100**	**150**	**200**	**0**	**50**	**100**	**150**	**200**
0	25.000	25.000	25.000	25.000	25.000	25.000	25.000	25.000	25.000	25.000
5	26.284	31.959	32.277	32.283	33.239	26.284	32.614	32.967	32.974	34.060
10	26.649	48.288	53.072	53.567	56.838	26.649	54.361	60.485	61.119	65.691
15	27.117	95.207	126.057	133.130	148.398	27.117	139.609	194.726	207.672	239.036
20	27.718	296.895	527.433	621.279	755.096	27.718	793.235	1610.555	1974.865	2563.336

4.4 Simulation IV

We compare the biomass concentrations in the stream at different velocities of 0.05, 0.35, and 0.65 m/s, along with nitrogen concentrations of 20, 300, 600, and 1200 mg/L, while considering spatial measurements taken at 10 and 20 d.

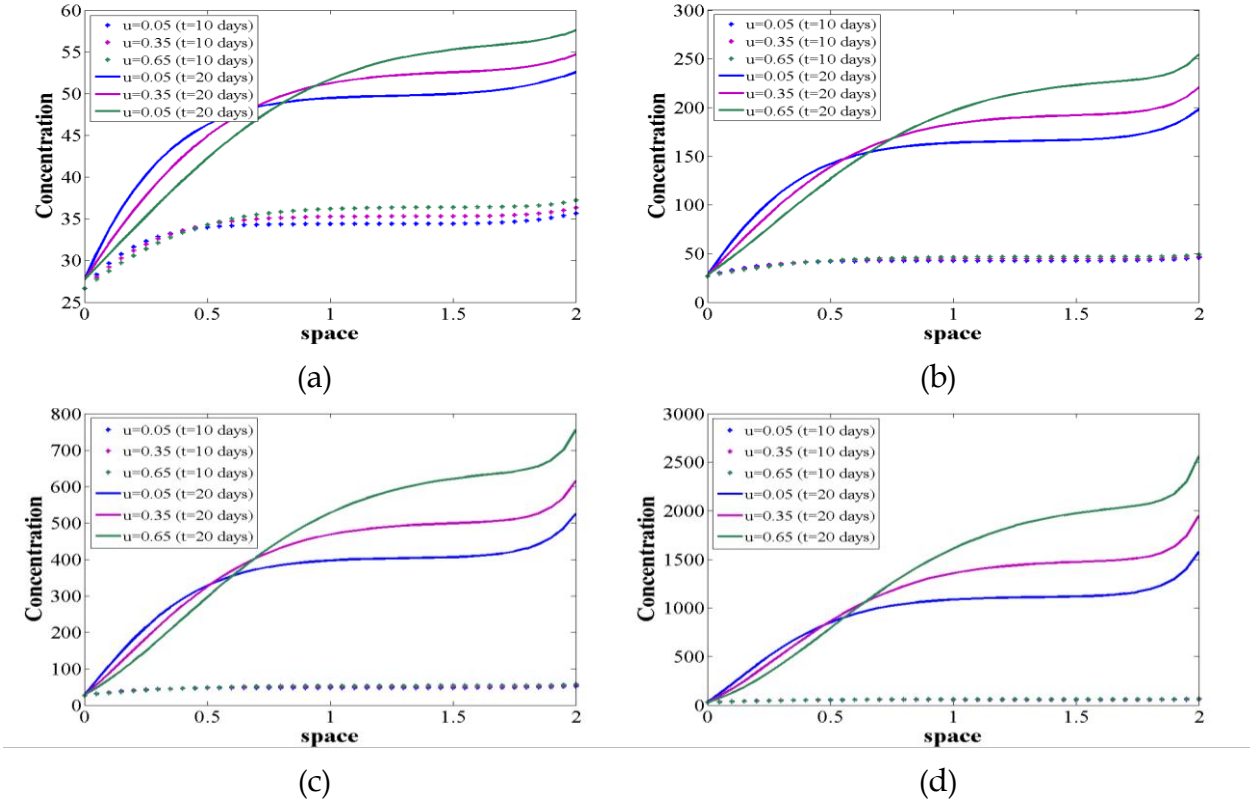

Figure 8. Comparison of the simulated solutions of biomass concentrations (mg/L) through spatial measurements at 10 and 20 d at different steam velocities of 0.05, 0.35, and 0.65 m/s for different nitrogen levels of (a) $C_n = 20$ mg/L, (b) $C_n = 300$ mg/L, (c) $C_n = 600$ mg/L, and (d) $C_n = 1200$ mg/L.

4.5 Simulation V

We compare the biomass concentrations in the stream at different velocities of 0.05, 0.35, and 0.65 m/s, along with nitrogen concentrations of 20, 300, 600, and 1200 mg/L, while considering temporal measurements taken at 10 and 20 d.

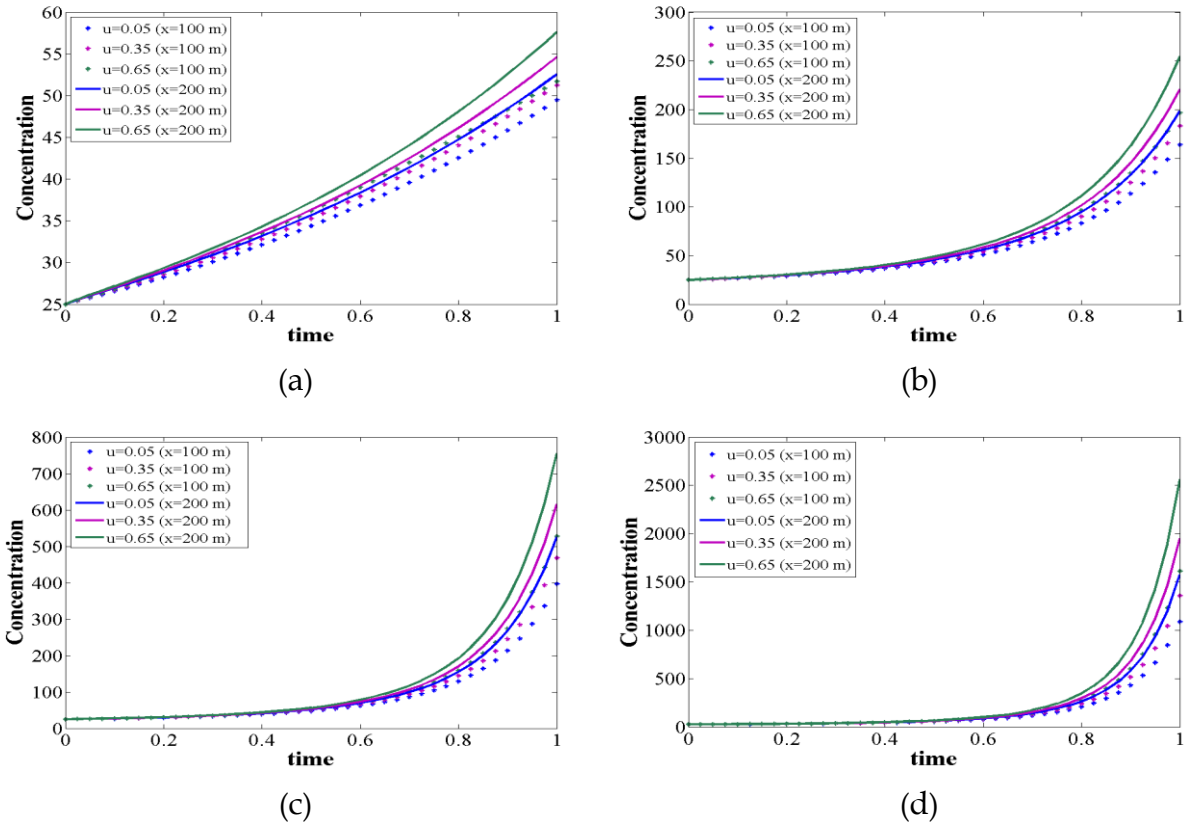

Figure 9. Comparison of the simulated solutions of biomass concentrations (mg/L) through temporal measurements at 100 and 200 m. at different steam velocities of 0.05, 0.35, and 0.65 m/s for different nitrogen levels of (a) $C_n = 20$ mg/L, (b) $C_n = 300$ mg/L, (c) $C_n = 600$ mg/L, and (d) $C_n = 1200$ mg/L.

5. Discussion

For performing numerical results from simulation studies, we simulate biomass concentrations at water flow velocities of 0.05, 0.35, and 0.65 m/s, corresponding to nitrogen levels of 20, 300, 600, and 1200 mg/L, as detailed: Figure 2 to Figure 7 and Table 2 to Table 7 illustrate Simulation I to Simulation III, showing that all three simulations show the direction of microalgae growth in the same way, wherein biomass concentration levels correlate with water flow velocity and nitrogen concentration levels, and alterations in biomass concentration levels would be enhanced to follow the distance and duration, as microalgae progressively assimilate nitrogen, leading to a continuous increase in biomass concentration levels. Simulation IV, depicted in Figure 8, illustrates the relationship between distance and varying water flow velocities concerning nitrogen concentration levels. At a low velocity of 0.05 m/s, the initial

distance, which is the result of increased biomass concentrations due to the slow water flow, accumulates higher nitrogen concentrations. Therefore, facilitating enhanced nitrogen uptake by microalgae at medium (0.35 m/s) and high velocities (0.65 m/s), biomass concentrations at 0.35 m/s are greater than those at 0.65 m/s. After some distance at a flow velocity of 0.05 m/s, biomass concentration levels declined as there was an accumulation of nitrogen concentrations decreasing, while at flow velocities of 0.35 m/s and 0.65 m/s, biomass concentration levels increased. The rapid flow led to the accumulation of nitrogen concentrations, which increased nitrogen uptake by microalgae. Simulation V, illustrated in Figure 9, compares the temporal aspect of biomass concentration levels across various water flow velocities. As time progressed, biomass concentration levels increased due to increased nitrogen accumulation, which in turn enhanced the nitrogen uptake by microalgae, thereby elevating biomass concentration levels. This increase is contingent upon water flow velocities of 0.05, 0.35, and 0.65 m/s and nitrogen concentration levels of 20, 300, 600, and 1200 mg/L, respectively.

6. Conclusion

In this study, we used Saulyev technique from the finite difference approach to develop a dynamic model for microalgae growth based on nitrogen removal along the stream. The biomass concentration levels that arise from the interaction between nitrogen concentration levels in agricultural wastewater areas and water flow velocities are displayed in the numerical simulations. The performance results in a low velocity, which causes high nitrogen concentrations to build up due to the initial distance, the slow water flow, and the ensuing higher biomass concentrations. Conversely, at high velocity, a decrease in nitrogen uptake by microalgae reduces biomass concentration. After a period at low velocity, the levels of biomass concentration decreased as nitrogen concentrations accumulated, whereas at high velocity, the levels of biomass concentration rose. The fast flow caused nitrogen concentrations to build up, which in turn enhanced microalgae's intake of nitrogen. Furthermore, biomass concentration levels are dependent on nitrogen concentration levels, meaning that higher nitrogen concentrations result in higher biomass concentration levels. Thus, the biomass concentration levels are influenced by the various water flow velocities and nitrogen concentration levels. In this simulation, we created a basic model that explains a real-world use of microalgae that allows pollution removal and active self-purification management. The model's adaptability to streams with varying features was demonstrated. The model is consistent and can be used to generate scenarios as part of a

general strategy to conserve or improve the management of water quality and be cost-efficient and environmentally friendly in wastewater treatment in agricultural wastewater areas. This is because flow velocities and nitrogen concentration levels are important factors in shaping the model response and must take into account microalgae growth to control biomass concentration. This makes pollution prevention necessary.

Conflicts of Interest: The authors declare that there are no conflicts of interest regarding the publication of this paper.

References

[1] N.M. Sunar, N.F.N. Abdullah, P.A. Gani, H.M.M. Peralta, A. Khalid, Extraction of Microalgae Miomass via Domestic Wastewater Phycoremediation, Fuel Mix. Form. Combust. Process. 1 (2019), 7.

[2] Z. KILIÇ, Water Pollution: Causes, Negative Effects and Prevention Methods, Istanb. Sabahattin Zaim Univ. J. Inst. Sci. Technol. 3 (2021), 129-132. https://doi.org/10.47769/izufbed.862679.

[3] M. Bystricky, C. Furrer, C. Ritzel, T. Nemecek, G. Gaillard, Effects of Water Protection Measures in Agriculture on the Environmental Impacts of the Swiss Food Sector, J. Clean. Prod. 466 (2024), 142819. https://doi.org/10.1016/j.jclepro.2024.142819.

[4] M. Ranjitham, N.V. Manjunath, G. Bharath, R.U. Deepak, R. Desika, An Overview of Agricultural Pollution: An Emerging Issue, Int. Res. J. Eng. Technol. 7 (2020), 1774-1776.

[5] R.M. Madjar, G.V. Scăeţeanu, M.A. Sandu, Nutrient Water Pollution from Unsustainable Patterns of Agricultural Systems, Effects and Measures of Integrated Farming, Water 16 (2024), 3146. https://doi.org/10.3390/w16213146.

[6] C.I. Ludemann, N. Wanner, P. Chivenge, A. Dobermann, R. Einarsson, P. Grassini, F.N. Tubiello, A Global FAOSTAT Reference Database of Cropland Nutrient Budgets and Nutrient Use Efficiency (1961–2020): Nitrogen, Phosphorus and Potassium, Earth Syst. Sci. Data 16 (2024), 525–541.

[7] I. Zahoor, A. Mushtaq, Water Pollution from Agricultural Activities: A Critical Global Review, Int. J. Chem. Biochem. Sci. 23 (2023), 164–176.

[8] M. Sarwar, Harmful Effects of Intensive Nitrogen Fertilizer Usage to Humans and Managing of Risks, Spec. J. Agric. Sci. 4 (2018), 9–15.

[9] G. Mancuso, G.F. Bencresciuto, S. Lavrnić, A. Toscano, Diffuse Water Pollution from Agriculture: A Review of Nature-Based Solutions for Nitrogen Removal and Recovery, Water 13 (2021), 1893. https://doi.org/10.3390/w13141893.

[10] M. Ranjitham, N.V. Manjunath, G. Bharath, R.U. Deepak, R. Desika, An Overview of Agricultural Pollution: An Emerging Issue, Int. Res. J. Eng. Technol. 7 (2020), 1774–1776.

[11] A.Q. Mugheri, Numerical Simulation of One-Dimensional Advection Diffusion Equation by New Hybrid Explicit Finite Difference Schemes, Quaid-e-Awam Univ. Res. J. Eng. Sci. Technol. 21 (2023), 54-62. https://doi.org/10.52584/qrj.2101.07.

[12] W. Klaychang, N. Pochai, Implicit Finite Difference Simulation of Water Pollution Control in a Connected Reservoir System, IAENG Int. J. Appl. Math. 46 (2016), 47–57.

[13] K. Suebyat, N. Pochai, A Numerical Simulation of a Three-Dimensional Air Quality Model in an Area Under a Bangkok Sky Train Platform Using an Explicit Finite Difference Scheme, IAENG Int. J. Appl. Math. 47 (2017), 1–6.

[14] P. Oyjinda, N. Pochai, Numerical Simulation to Air Pollution Emission Control Near an Industrial Zone, Adv. Math. Phys. 2017 (2017), 5287132. https://doi.org/10.1155/2017/5287132.

[15] P. Samalerk, N. Pochai, Numerical Simulation of a One-Dimensional Water-Quality Model in a Stream Using a Saulyev Technique with Quadratic Interpolated Initial-Boundary Conditions, Abstr. Appl. Anal. 2018 (2018), 1926519. https://doi.org/10.1155/2018/1926519.

[16] A. Vongkok, N. Pochai, Numerical Models of Nitrogen Compound Measurements in a Stream with Removal Mechanism Using Saulyev Technique with Cubic Spline Interpolation, J. Interdiscip. Math. 22 (2019), 1235-1275. https://doi.org/10.1080/09720502.2019.1668153.

[17] A. Vongkok, N. Pochai, Numerical Simulations for Reactive Nitrogen Compounds Pollution Measurements in a Stream Using Saulyev Method, Ital. J. Pure Appl. Math. 43 (2020), 552–582.

[18] J. Yang, C. Lee, S. Kwak, Y. Choi, J. Kim, A Conservative and Stable Explicit Finite Difference Scheme for the Diffusion Equation, J. Comput. Sci. 56 (2021), 101491. https://doi.org/10.1016/j.jocs.2021.101491.

[19] S. Pourghanbar, J. Manafian, M. Ranjbar, A. Aliyeva, Y.S. Gasimov, An Efficient Alternating Direction Explicit Method for Solving a Nonlinear Partial Differential Equation, Math. Probl. Eng. 2020 (2020), 9647416. https://doi.org/10.1155/2020/9647416.

[20] P. Othata, N. Pochai, A One-Dimensional Mathematical Simulation to Salinity Control in a River with a Barrage Dam Using an Unconditionally Stable Explicit Finite Difference Method, Adv. Differ. Equ. 2019 (2019), 203. https://doi.org/10.1186/s13662-019-2106-4.

[21] P. Samalerk, N. Pochai, A Saulyev Explicit Scheme for an One-Dimensional Advection-Diffusion-Reaction Equation in an Opened Uniform Flow Stream, Thai J. Math. 18 (2020), 677–683.

[22] S. Manilam, N. Pochai, A Non-Dimensional Mathematical Model of Shoreline Evolution with a Groin Structure Using an Unconditionally Stable Explicit Finite Difference Technique, IAENG Int. J. Appl. Math. 52 (2022), 473.

[23] U.A.F.M. Sadiq, M.E. Yow, S.S. Jamaian, The Extended Monod Model for Microalgae Growth and Nutrient Uptake in Different Wastewaters, Int. J. Eng. Technol. 7 (2018), 200-204. https://doi.org/10.14419/ijet.v7i4.30.22120.